nature medicine

Using iPSC-derived neurons to uncover cellular phenotypes associated with Timothy syndrome

Sergiu P Paşca[1], Thomas Portmann[1,7], Irina Voineagu[2,7], Masayuki Yazawa[1,7], Aleksandr Shcheglovitov[1], Anca M Paşca[1], Branden Cord[3], Theo D Palmer[3], Sachiko Chikahisa[4,5], Seiji Nishino[4], Jonathan A Bernstein[6], Joachim Hallmayer[4], Daniel H Geschwind[2] & Ricardo E Dolmetsch[1]

Monogenic neurodevelopmental disorders provide key insights into the pathogenesis of disease and help us understand how specific genes control the development of the human brain. Timothy syndrome is caused by a missense mutation in the L-type calcium channel $Ca_v1.2$ that is associated with developmental delay and autism[1]. We generated cortical neuronal precursor cells and neurons from induced pluripotent stem cells derived from individuals with Timothy syndrome. Cells from these individuals have defects in calcium (Ca^{2+}) signaling and activity-dependent gene expression. They also show abnormalities in differentiation, including decreased expression of genes that are expressed in lower cortical layers and in callosal projection neurons. In addition, neurons derived from individuals with Timothy syndrome show abnormal expression of tyrosine hydroxylase and increased production of norepinephrine and dopamine. This phenotype can be reversed by treatment with roscovitine, a cyclin-dependent kinase inhibitor and atypical L-type–channel blocker[2–4]. These findings provide strong evidence that $Ca_v1.2$ regulates the differentiation of cortical neurons in humans and offer new insights into the causes of autism in individuals with Timothy syndrome.

Human genetic studies have implicated voltage-gated calcium channels, in particular the L-type channel $Ca_v1.2$, in the development of psychiatric diseases such as autism[5], bipolar disorder[6] and schizophrenia[7]. Although calcium influx through these channels is crucial for a variety of neuronal processes including regulation of gene expression[8], the cellular defects caused by mutations in these channels and how they lead to psychiatric symptoms is unknown. Timothy syndrome is caused by a point mutation in an alternatively spliced exon of *CACNA1C*, the gene that encodes the α_1 subunit of $Ca_v1.2$ (ref. 1). This mutation leads to decreased calcium- and voltage-dependent inactivation of the channel[1,9]. Individuals with Timothy syndrome suffer from cardiac arrhythmia, hypoglycemia and global developmental delay. Over 60% of individuals with Timothy syndrome also fulfill the criteria for an autism spectrum disorder (ASD)[1] making Timothy syndrome one of the most penetrant monogenic forms of autism.

To determine the cellular consequences of the mutation causing Timothy syndrome, we used somatic cell reprogramming[10,11] to generate induced pluripotent stem cells (iPSCs) from individuals with Timothy syndrome (see **Supplementary Figs. 1** and **2**, **Supplementary Methods** and ref. 12 for characterization of these cells and **Supplementary Table 1** for a list of the cell lines used in each experiment). We differentiated the iPSC lines into neuronal precursor cells (NPCs) and neurons using conditions that favor the generation of cortical neurons[13–15] (see **Fig. 1**, **Supplementary Fig. 3**, Online Methods and **Supplementary Methods** for details about the *in vitro* differentiation process). To identify the types of cells in these cultures, we used Fluidigm Dynamic Arrays[16] to measure the expression of region-specific and cell-type–specific marker genes in single cells (**Fig. 1b** and **Supplementary Table 2**). We verified the reliability and accuracy of this method in measuring single-cell gene expression in a variety of ways (ref. 17, **Supplementary Figs. 4** and **5** and **Supplementary Methods**). Overall, in cultures derived from control subjects, 64.9% of the cells at day 45 of differentiation *in vitro* expressed a neuronal marker (*MAP2* or *NCAM*). Individual neurons expressed combinations of genes that indicate their neurotransmitter identity and cortical-layer specificity (**Fig. 1b**). A substantial number of neurons expressed excitatory markers such as those encoded by *SLC17A7* (also known as *VGLUT1*) and *SLC17A6* (also known as *VGLUT2*) along with the dopamine receptor encoded by *DRD2*, whereas other neurons expressed the inhibitory markers encoded by *GAD2* (also known as *GAD65*), *GAD1* (also known as *GAD67*) and *SLC32A1* (also known as *VGAT*).

We sought to determine the cortical layer identity of the neurons in these iPSC-derived cultures, by examining the distribution of layer-specific marker genes using single cell Fluidigm arrays. We chose markers that have been characterized immunohistochemically in human brain (refs. 18,19) (**Fig. 1c**). We classified cells as

[1]Department of Neurobiology, Stanford University School of Medicine, Stanford, California, USA. [2]Department of Neurology and Program in Neurogenetics, David Geffen School of Medicine, University of California, Los Angeles, California, USA. [3]Stanford Institute for Stem Cell Biology and Regenerative Medicine and Department of Neurosurgery, Stanford School of Medicine, Stanford, California, USA. [4]Department of Psychiatry and Behavioral Science, Stanford University School of Medicine, Stanford, California, USA. [5]Department of Integrative Physiology, Institute of Health Biosciences, The University of Tokushima Graduate School, Tokushima, Japan. [6]Department of Pediatrics, Stanford University School of Medicine, Stanford, California, USA. [7]These authors contributed equally to this work. Correspondence should be addressed to R.E.D. (ricardo.dolmetsch@stanford.edu).

Received 8 July; accepted 18 October; published online 27 November 2011; doi:10.1038/nm.2576

lower-layer cortical neurons if they expressed *ETV1*, *FOXP1* or both in addition to *NCAM* or *MAP2*. We classified these cells as upper-layer cortical neurons if they failed to express either *ETV1* or *FOXP1* but expressed at least one cortical layer marker such as *CUX1*, *SATB2*, *BCL11B* (also called *CTIP2*) or *RELN*. We found that ~85% of the neurons derived from control subjects could be classified as lower cortical-layer neurons while the remaining 15% were upper cortical cells (**Fig. 1d**). Within the population of lower cortical neurons, we found a group of cells that co-expressed *CTIP2* (*BCL11B*) in addition to *ETV1* and/or *FOXP1* (**Fig. 1e**). *In vivo*, this distribution of markers defines a population of subcortical projection neurons[20–22]. Our cultures also contained a population of cells that expressed *SATB2* and *ETV1* and/or *FOXP1*, which *in vivo* defines a group of neurons that projects to distant cortical regions through the corpus callosum[20–22] (**Fig. 1d**). A notable finding from this analysis was the reproducibility of neuronal differentiation across multiple iPSC lines and individuals (the average s.d. for the proportion of cells expressing a particular marker was 4.5%), indicating that this process is highly reproducible *in vitro* and that single-cell analysis of gene expression can be used to identify abnormalities in neuronal differentiation.

The ability to generate well-defined populations of NPCs and neurons from iPSCs prompted us to ask whether we could identify cellular phenotypes associated with Timothy syndrome. We examined the total number of neurons (**Supplementary Fig. 5**) and the proliferation

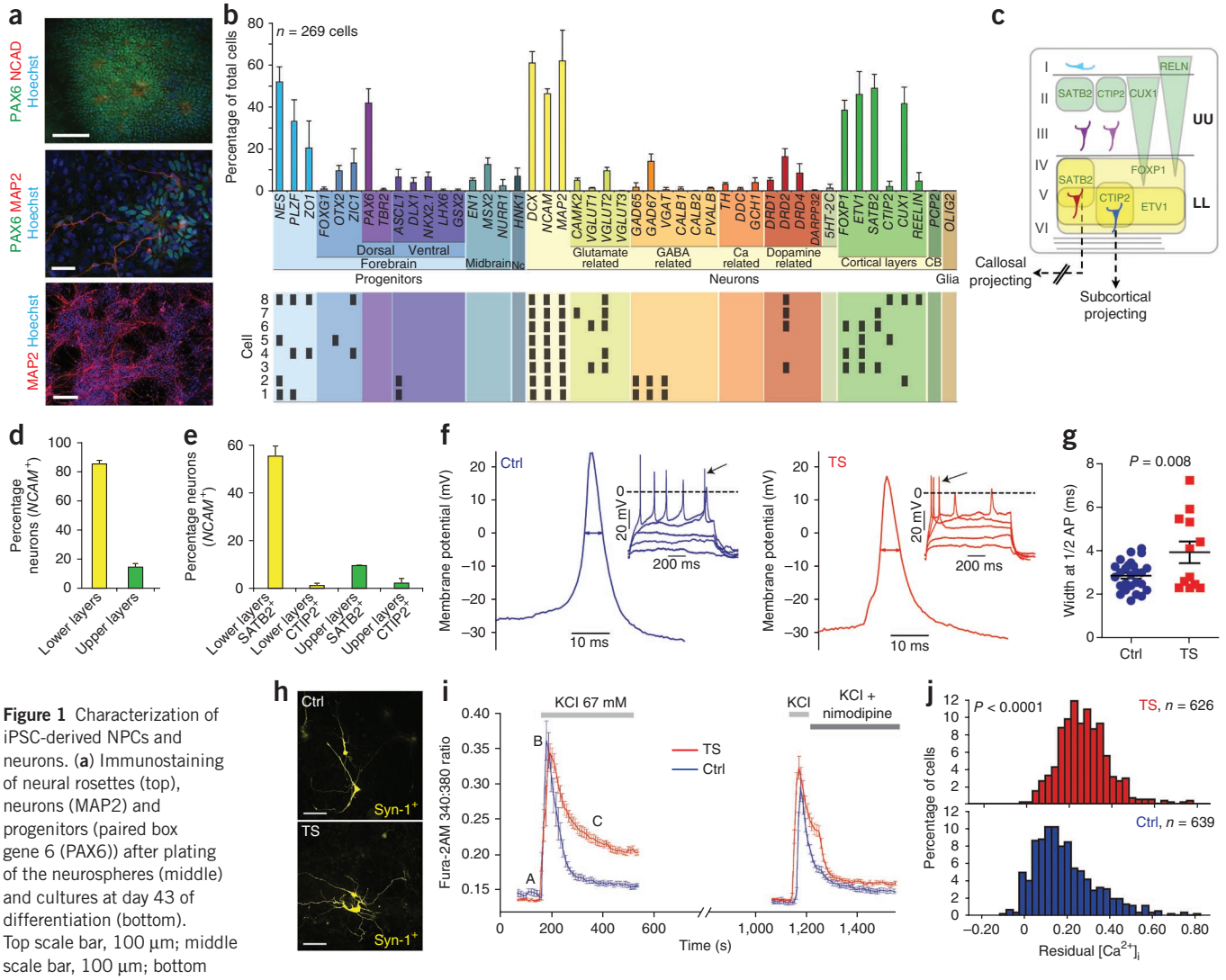

Figure 1 Characterization of iPSC-derived NPCs and neurons. (**a**) Immunostaining of neural rosettes (top), neurons (MAP2) and progenitors (paired box gene 6 (PAX6)) after plating of the neurospheres (middle) and cultures at day 43 of differentiation (bottom). Top scale bar, 100 µm; middle scale bar, 100 µm; bottom scale bar, 200 µm. The middle image is from a Timothy syndrome–derived culture, and the other two are from cultures derived from control individuals. (**b**) Single-cell gene expression analysis of the population of cells after 45 d of differentiation. Shown are the proportion of cells that expressed a cell-specific marker (data are mean ± s.e.m.; $n = 269$ cells from three control iPSC lines). At the bottom are gene expression profiles of single neurons. (**c**) A scheme illustrating marker gene expression in the upper layers (UL) and lower layers (LL) of the human cortex. (**d**) Fraction of neurons (*NCAM*$^+$) expressing lower-layer (*FOXP1*$^+$*ETV1*$^+$) or upper-layer (*FOXP1*$^-$*ETV1*$^-$) cortical markers (data are mean ± s.e.m.; $n = 116$ cells from three controls iPSC lines). (**e**) Fraction of subpopulations of upper-layer and lower-layer neurons (*NCAM*$^+$) expressing *CTIP2* (*BCL11B*) or *SATB2*. (**f**) Representative current-clamp recordings (with a holding potential of –65 mV, 1 s current pulses and ΔI_{inj} = 5–10 pA) from Timothy syndrome (TS)-derived and control-derived neurons. (**g**) Action potentials (APs) recorded from the Timothy syndrome–derived neurons were significantly wider than those from control-derived neurons. (**h**) Representative images of control-derived (Ctrl) and Timothy syndrome (TS)-derived neurons expressing YFP under the control of the synapsin-1 (syn-1$^+$) promoter (scale bars, 50 µm). (**i**) Average $[Ca^{2+}]_i$ measurements in synapsin-1–expressing neurons depolarized twice with 67 mM KCl and treated with 5 µM nimodipine ($n = 10$ neurons for Timothy syndrome and $n = 9$ neurons for control). (**j**) Histogram of residual $[Ca^{2+}]_i$ in single cells, computed by dividing the plateau calcium level by the peak calcium elevation ((C – A) / (B – A) as shown in **i**; three Timothy syndrome lines and three control lines; *t* test, $P < 0.0001$; see also **Supplementary Fig. 8**).

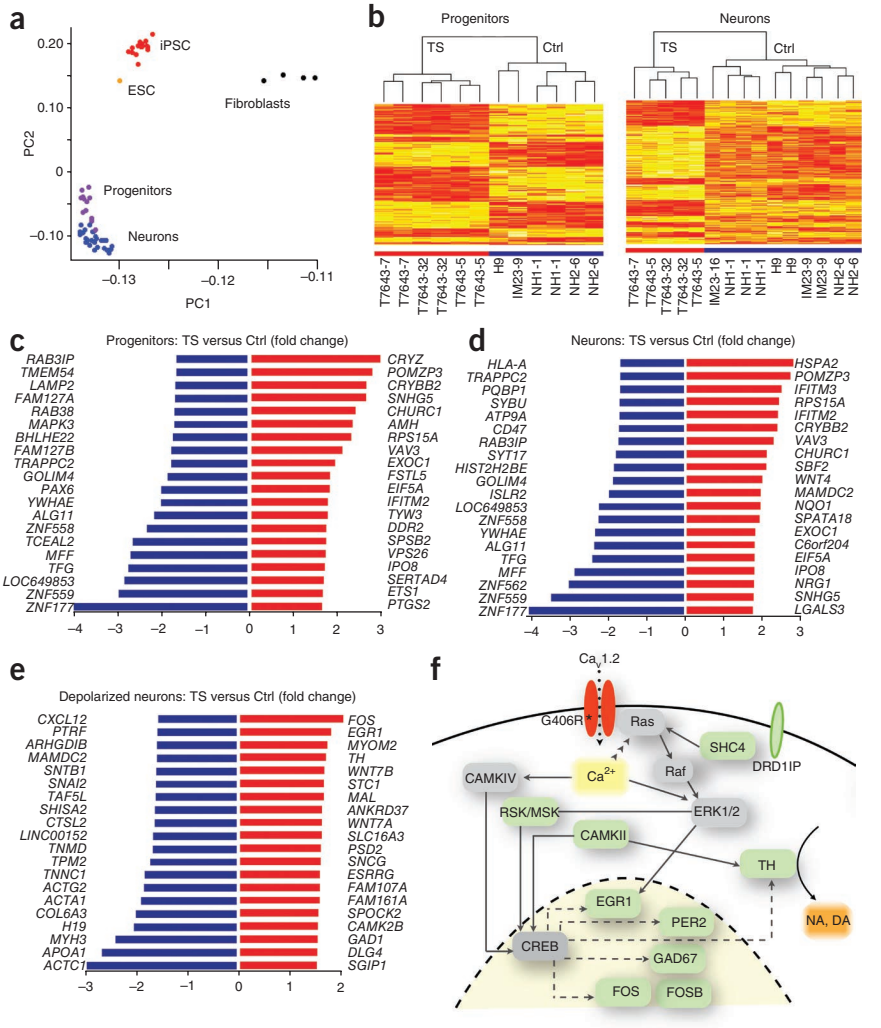

Figure 2 Characterization of NPCs and neurons by genome-wide microarrays. (**a**) Principal component analysis of whole-genome gene expression profiles for fibroblasts, iPSCs, embryonic stem cells (ESCs), NPCs and neurons showing clustering of cell types based on the first two principal components (PC1 and PC2). (**b**) Heatmaps depicting the expression of genes differentially expressed between Timothy syndrome and control NPCs and neurons. Each column represents an independent differentiation of an iPSC line. Genes that are highly expressed in Timothy syndrome cells relative to controls are shown in red. The dendrograms show the hierarchical clustering of samples based on differentially expressed genes. (**c**,**d**) A list of the top 20 genes showing the greatest differences (upregulated genes are shown in red and downregulated genes are shown in blue) in expression between Timothy syndrome and control cells (**c** shows progenitors and **d** shows neurons). (**e**) Differentially expressed genes in Timothy syndrome-derived neurons relative to control-derived neurons after electrical stimulation. (**f**) A scheme illustrating interactions between a subset of calcium-regulated proteins that are upregulated in Timothy syndrome (green). G406R indicates the Timothy syndrome mutation (a substitution of glycine with arginine at residue 406).

(**Supplementary Fig. 6a**) and migration (**Supplementary Fig. 6b**,**c**) of NPCs, but we found no differences between cultures from controls and those from individuals with Timothy syndrome. We next used patch-clamp recording and calcium imaging to assess the physiological properties of neurons generated from the iPSC lines (**Fig. 1f**). Fifty-seven percent of the iPSC-derived cells fired mature action potentials (**Supplementary Fig. 7**). A comparison of Timothy syndrome and control neurons did not reveal any significant differences in the action potential threshold or amplitude, resting membrane potential, input resistance or capacitance (**Supplementary Table 3**). However, the action potentials of Timothy syndrome neurons were approximately 37% wider at the midpoint than those of controls (3.92 ms ± 0.49 ms (mean ± s.e.m.) for Timothy syndrome compared to 2.86 ms ± 0.12 ms for control; $P = 0.008$), which is consistent with a loss of channel inactivation in Timothy syndrome (**Fig. 1f**,**g**) and is similar to the defect we observed in iPSC-derived cardiomyocytes from individuals with Timothy syndrome[12].

We next examined the intracellular calcium ($[Ca^{2+}]_i$) signals in Timothy syndrome and control NPCs and neurons using the calcium indicator Fura-2 and time-lapse video microscopy. Because the cultures contained a mixed population of neurons and NPCs, we first measured $[Ca^{2+}]_i$ in mature neurons expressing a yellow fluorescent protein (YFP) reporter gene under the control of the synapsin-1 promoter (**Fig. 1h**). In Timothy syndrome cells, we observed a significant increase in the sustained $[Ca^{2+}]_i$ rise after depolarization that was abolished by treatment with the L-type calcium channel blocker nimodipine (**Fig. 1i**). We observed this increased $[Ca^{2+}]_i$ rise also in nonlabeled Timothy syndrome neurons derived from multiple lines and multiple independent differentiations (**Fig. 1j** and **Supplementary Fig. 8a**,**b**). Similarly, we observed increased $[Ca^{2+}]_i$ elevations in Timothy syndrome NPCs (**Supplementary Fig. 8c**,**d**). Taken together, these results provide strong evidence that NPCs and neurons derived from individuals with Timothy syndrome have defects in action potential firing and $[Ca^{2+}]_i$ signaling.

$Ca_V1.2$ has a key role in regulating activity-dependent gene expression in the nervous system[8]. We therefore used Illumina microarrays to compare the gene expression profiles of Timothy syndrome and control NPCs and neurons (**Fig. 2a–d**). Hierarchical clustering based on differentially expressed genes showed that Timothy syndrome cells clustered separately from controls. The expression of 211 genes (126 upregulated and 85 downregulated) in neurons and 136 genes (58 upregulated and 78 downregulated) in NPCs was substantially altered in Timothy syndrome cells (**Fig. 2c**,**d** and **Supplementary Table 4**). Of the genes with altered expression in Timothy syndrome neurons, 11 were previously implicated in either ASD or intellectual disability[23,24] (**Supplementary Table 5**).

We also identified 223 genes (135 upregulated and 88 downregulated) whose expression was altered in Timothy syndrome relative to control neurons after depolarization. A number of the genes that were altered in Timothy syndrome cells are linked to Ca^{2+}-dependent regulation of the transcription factor cAMP response-element binding (CREB) (**Fig. 2e**,**f**), including *RPS6KA1-SIK1* (also known as *RSK-MSK*) and *CAMKII*. Other genes, such as *EGR1*, *FOS*, *FOSB*, *GAD1* and *TH*, are downstream targets of *CREB*. In addition to *TH*,

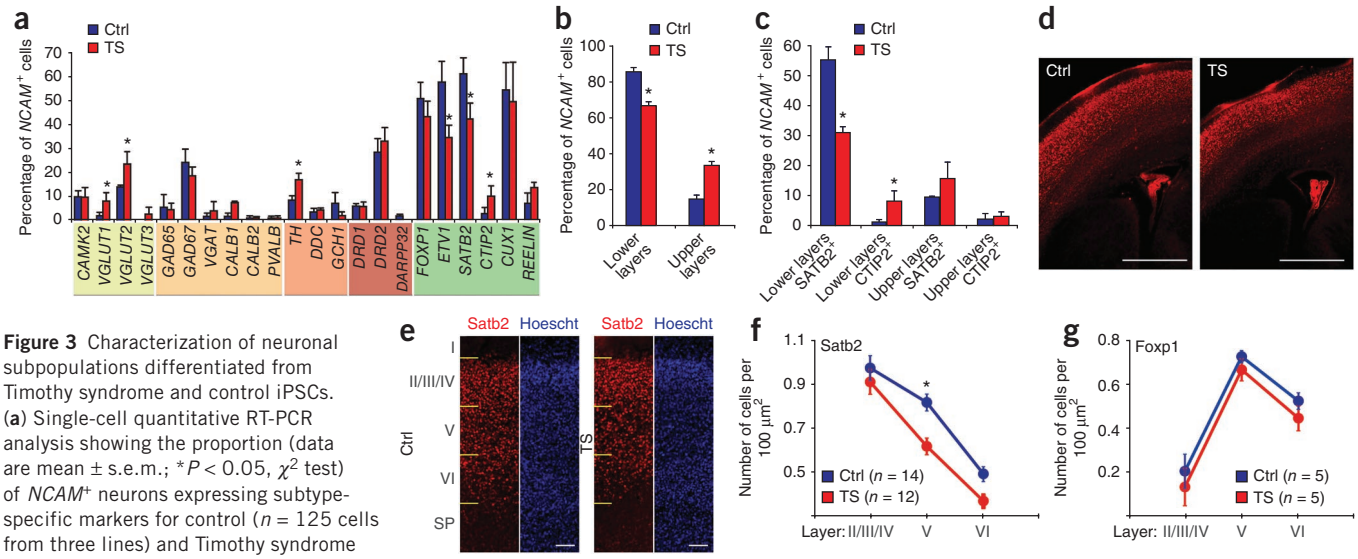

Figure 3 Characterization of neuronal subpopulations differentiated from Timothy syndrome and control iPSCs. (**a**) Single-cell quantitative RT-PCR analysis showing the proportion (data are mean ± s.e.m.; $^*P < 0.05$, χ^2 test) of *NCAM*$^+$ neurons expressing subtype-specific markers for control ($n = 125$ cells from three lines) and Timothy syndrome ($n = 140$ cells from three lines) cultures. (**b**) Fraction of neurons expressing upper- and lower-layer cortical makers in Timothy syndrome–derived ($n = 125$ cells) and control-derived ($n = 116$ cells) cortical cultures (data are mean ± s.e.m.; $^*P < 0.05$, χ^2 test). (**c**) Fraction of neurons expressing *SATB2* and *CTIP1* (*BCL11B*) and either lower- or upper-layer cortical markers in Timothy syndrome and control cultures (data are mean ± s.e.m.; $^*P < 0.05$, χ^2 test). (**d**) A magnified (×50) image of cortical sections stained for Satb2 from a control mouse and a mouse expressing the Timothy syndrome channel in the forebrain. Scale bar, 500 µm. (**e**) Image of cortical sections stained for Satb2 from a control and a Timothy syndrome mouse at postnatal day 0.5 (scale bar, 50 µm). (**f**) Measurement of the number of Satb2$^+$ cortical neurons in cortical sections from Timothy syndrome and control mice (data are mean ± s.e.m.; $n = 12$ mice for Timothy syndrome and $n = 14$ mice for the control; two-way ANOVA, $P = 0.001$; $^*P < 0.05$ in the Bonferroni *post hoc* analysis). (**g**) Distribution of Foxp1$^+$ neurons in cortical sections from Timothy syndrome and control mice (data are mean ± s.e.m.; $n = 5$ mice per group; two-way ANOVA, $P > 0.05$).

which encodes the rate-limiting enzyme in the production of dopamine and norepinephrine, *CALY* (encoding calcyon and also known as *DRD1IP*), another gene involved in dopamine signaling, was also upregulated in Timothy syndrome neurons. These results suggest that the mutation that causes Timothy syndrome leads to the misregulation of Ca^{2+}-dependent gene expression and perturbs catecholamine signaling.

To determine whether the Timothy syndrome mutation leads to defects in neuronal differentiation, we used Fluidigm arrays to study the identity of cells generated from individuals with Timothy syndrome compared to controls (**Fig. 3a**). We found a significant decrease in the fraction of neurons expressing lower-layer markers in Timothy syndrome cells relative to controls (66.7% of neurons expressed these markers in Timothy syndrome cells compared to 85.5% in controls; $P < 0.001$; **Fig. 3b**) and an increase in the fraction of neurons expressing upper-layer markers (33.3% in Timothy syndrome cells compared to 14.5% in controls; $P = 0.002$; **Fig. 3b**). A significantly lower proportion of Timothy syndrome cells expressing lower-layer markers (**Fig. 3c**) expressed *SATB2* (31.0% of Timothy syndrome cells compared to 55.3% of controls; $P < 0.001$), and a significantly higher proportion expressed *CTIP2* (*BCL11B*) relative to controls (8.0% of Timothy syndrome cells compared to 1.0% of controls; $P = 0.01$). Because *SATB2* is both necessary and sufficient for the specification of callosal projection neurons[20,21], this finding suggests that the Timothy syndrome mutation decreases the fraction of callosal projection neurons and increases the number of cells that project to subcortical structures.

To provide additional support for these results *in vivo*, we measured Satb2 expression in a transgenic mouse expressing $Ca_v1.2$ carrying the mutation associated with Timothy syndrome type 1, expressed in the forebrain under the control of the *Foxg1* promoter (**Supplementary Fig. 9**). Timothy syndrome–transgenic mice had a reduced number of cells expressing Satb2 in the lower cortical layers (**Fig. 3d–f**), whereas Foxp1 expression (**Fig. 3g**) and the total number of neurons expressing Rbfox3 (also known as NeuN) in the cortex were unchanged. We therefore conclude that the Timothy syndrome mutation alters *SATB2* expression both *in vitro* and *in vivo*. Notably, we did not observe an increase in the number of cells expressing Ctip2 (Bcl11b) in the mice expressing the Timothy syndrome channel. This could be either because of differences between *in vivo* and *in vitro* neuronal differentiation or because of species-specific differences in CTIP2 (BCL11B) regulation. CTIP2 (BCL11B) is, in fact, expressed more broadly in humans than in mice, labeling cells in the subventricular zone as well as in cortical layers II and V in humans[25].

We also observed a significant increase in the fraction of cells that expressed *TH* in Timothy syndrome neuronal cultures (16.4% of Timothy syndrome cells expressed *TH* compared to 8.0% of controls; $P = 0.03$; **Fig. 3a**). This agrees with our earlier finding that genes involved in catecholamine synthesis are misregulated in Timothy syndrome (**Fig. 2e,f**). To determine whether the Timothy syndrome mutation alters the regulation of *TH*, we measured *TH* mRNA in Timothy syndrome and control neurons following electrical activation (**Fig. 4a**). After 9 h of stimulation, *TH* was downregulated in control neurons but was upregulated in Timothy syndrome neurons, indicating that the Timothy syndrome mutation prevents downregulation of TH in response to prolonged electrical activity.

To investigate whether this increase in *TH* mRNA has functional consequences, we measured expression of tyrosine hydroxylase (TH) protein using an antibody specific for TH. We found that 15.03% ± 0.92% (mean ± s.e.m., $n = 9$ differentiations) of the Timothy syndrome neurons expressed TH, whereas only 2.52% ± 0.62% (mean ± s.e.m., $n = 7$ differentiations) of the control cultures expressed the protein (**Fig. 4b–d**; *t* test, $P < 0.001$). Cultures generated from an individual with 22q11.2 deletion syndrome, which is another neurodevelopmental disorder, did not show increased expression of TH, indicating that

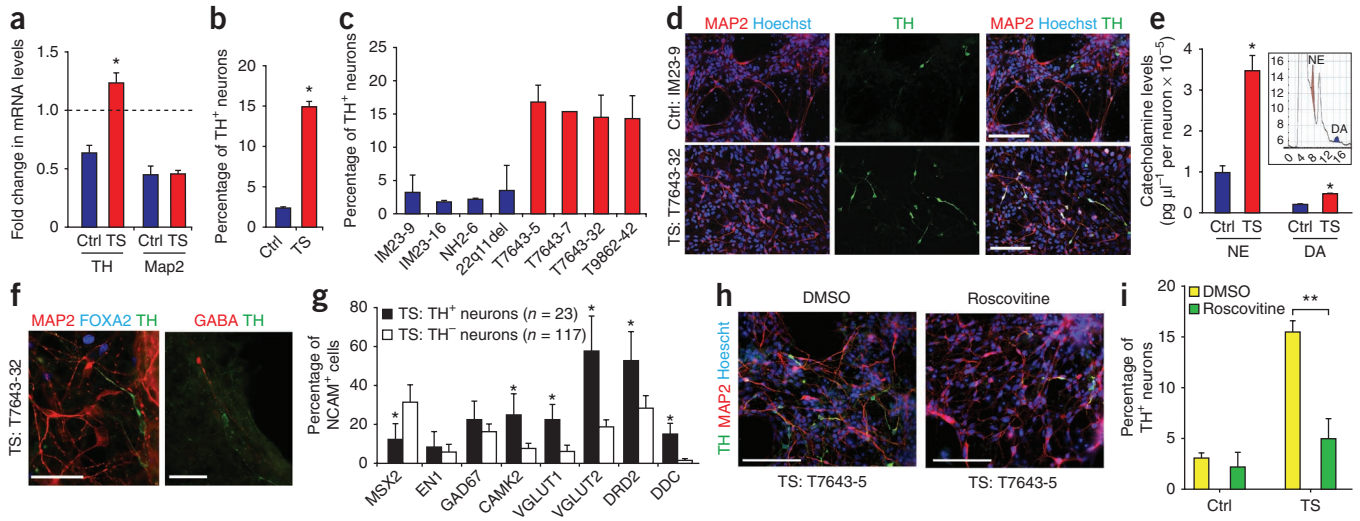

Figure 4 Abnormal expression of TH in iPSC-derived neurons from individuals with Timothy syndrome. (**a**) Fold changes in *TH* and *MAP2* mRNA levels in Timothy syndrome–derived and control-derived neurons after 9 h of depolarization with 67 mM KCl. (**b**) Proportion of TH^+ neurons in Timothy syndrome–derived neuronal cultures ($^*P < 0.001$, *t* test). (**c**) The proportion of TH^+ neurons (TH^+MAP2^+) is shown separately for three control lines from two healthy individuals (IM23-9, IM23-16 and NH2-6), one line derived from an individual with 22q11.2 deletion syndrome and four Timothy syndrome lines from two individuals (T7643-5, T7643-7 and T7643-32 for the first individual and T9862-42 for the second individual). (**d**) Representative images of neurons stained with antibodies specific to TH and MAP2 and with Hoechst 33258 (scale bars, 200 µm). (**e**) Norepinephrine (NE; $^*P = 0.004$) and dopamine (DA; $^*P = 0.001$) concentrations in media collected from Timothy syndrome–derived neuronal cultures relative to controls. The inset is an HPLC chromatogram showing the peaks for norepinephrine and dopamine. (**f**) TH^+ neurons (green) in Timothy syndrome cultures (the T7643-32 line is shown) were not immunostained by antibodies to FOXA2 (left, blue) or GABA (right, red). Scale bar, 50 µm. (**g**) The fraction of TH^+ or TH^- neurons derived from individuals with Timothy syndrome that co-express other neuronal marker genes (data are mean ± s.e.m.; $^*P < 0.05$, χ^2 test). (**h**) Cultures of Timothy syndrome neurons treated with roscovitine (15 µM at day 39 and 10 µM at day 41) or DMSO and stained with antibodies specific to TH and MAP2 at day 43 of differentiation. Scale bar, 200 µm. (**i**) Proportion of TH^+ neurons (TH^+MAP2^+) in control and Timothy syndrome cultures after treatment with roscovitine or DMSO (data are mean ± s.e.m.; two-way ANOVA, $^{**}P < 0.001$).

this defect is relatively specific for Timothy syndrome (**Fig. 4c**). To determine whether this change in TH protein caused an increase in the production of catecholamines, we used HPLC to measure the amount of norepinephrine and dopamine in the media collected from the neuronal cultures. We found that the Timothy syndrome neurons secreted 3.5× more norepinephrine ($34.7 \times 10^{-5} \pm 4.02 \times 10^{-5}$ pg µl^{-1} per neuron for Timothy syndrome compared to $9.79 \times 10^{-5} \pm 1.83 \times 10^{-5}$ pg µl^{-1} per neuron for controls; *t* test, $P = 0.004$) and 2.3× more dopamine ($4.56 \times 10^{-5} \pm 0.36 \times 10^{-5}$ pg µl^{-1} per neuron for Timothy syndrome compared to $2.05 \times 10^{-5} \pm 0.24 \times 10^{-5}$ pg µl^{-1} per neuron; *t* test, $P = 0.001$) than control lines, strongly suggesting that the Timothy syndrome mutation leads to increased TH expression and to an excess secretion of catecholamines (**Fig. 4e**).

We next investigated the cellular identity of neurons that produce TH in Timothy syndrome and control cultures. In both control and Timothy syndrome cultures, TH-expressing neurons were not stained with antibodies to forkhead box A2 (FOXA2) or engrailed homeobox 1 (EN1), markers of midbrain neurons, or to γ-aminobutyric acid (GABA), a marker for dopaminergic olfactory neurons in the forebrain (**Fig. 4f**). Using Fluidigm chip analysis, we found that TH expression was not confined to any specific class of neurons, although TH^+ neurons derived from individuals with Timothy syndrome were more likely to co-express excitatory markers and dopamine-related genes (**Fig. 4g**). This suggests that the Timothy syndrome channel does not promote a catecholaminergic cell fate but instead increases the expression of TH in a subpopulation of cortical cell types. Notably, we did not observe an increase in TH staining in the cortex of transgenic mice expressing the Timothy syndrome channel. This probably reflects the low homology between the promoter regions of mouse and human *TH* and differences in gene regulation[26,27].

Finally, to determine whether the increase in TH expression was reversible and was a result of L-type–channel activity, we treated 39-day-old iPSC-derived neurons from individuals with Timothy syndrome with L-type–channel blockers. The conventional L-type channel blocker nimodipine failed to reverse the excess expression of TH in neurons in these cells. However, treatment with roscovitine, a compound that increases inactivation of the L-type channel, caused a 68% reduction in the proportion of TH^+ neurons (**Fig. 4h,i**; $P < 0.01$ two-way analysis of variance (ANOVA); $n = 3{,}975$ neurons from three Timothy syndrome iPS lines and $n = 2{,}679$ from three control lines) without affecting the fraction of cells expressing MAP2. This is consistent with earlier studies of iPSC-derived cardiomyocytes[12] from individuals with Timothy syndrome, showing that roscovitine[2–4] can reduce the prolongation of the cardiac action potential in these cells. This result suggests that the increase in TH expression results from lack of inactivation of the channels containing the Timothy syndrome mutation and, further, that restoring channel inactivation in mature neurons can decrease the abnormal expression of TH in the cells of individuals with Timothy syndrome.

In this study, we show that iPSC-derived neurons from individuals with Timothy syndrome can be used to identify cellular phenotypes associated with a neurodevelopmental disorder. These findings provide insight both into the function of $Ca_v1.2$ in the developing human brain and its role in the pathogenesis of psychiatric diseases. We report an increase in the amplitude of Ca^{2+} elevations in Timothy syndrome NPCs and neurons, indicating that loss of inactivation in a single splice variant of $Ca_v1.2$ can have substantial effects on neuronal signaling. A consequence of this defect was a change in activity-dependent gene expression and an increase in cells producing norepinephrine and dopamine, consistent with previous experiments showing that dopaminergic specification is activity dependent[28]. The Timothy syndrome mutation also caused a decrease

in the proportion of cells expressing lower-cortical-layer markers and a decrease in the proportion of cells expressing markers for callosal projection neurons. Some, but not all, of these defects were recapitulated in a mouse expressing the channel with the Timothy syndrome mutation, suggesting that species-specific differences in gene regulation can change the cellular phenotypes associated with a disease[26,27]. A key question is whether these cellular defects help to explain the developmental delay and ASD seen in individuals with Timothy syndrome. The reduction in cortical projecting neurons in Timothy syndrome is consistent with the emerging view that ASDs arise from defects in connectivity between cortical areas[29,30] and agrees with studies that reported a decreased size of the corpus callosum in ASD[31]. Ectopic production of TH and a subsequent increase in catecholamine synthesis is consistent with findings from valproic-acid based models of ASD[32] and postmortem studies of individuals with schizophrenia[33]. As catecholamines have a key role in sensory gating and in social behavior, an increase in their synthesis could play a role in the pathophysiology of ASDs.

METHODS

Methods and any associated references are available in the online version of the paper at http://www.nature.com/naturemedicine/.

Accession codes. Microarray data are available in the Gene Expression Omnibus under accession code GSE25542.

Note: Supplementary information is available on the Nature Medicine website.

ACKNOWLEDGMENTS

We thank K. Timothy and the individuals with Timothy syndrome who participated in this study; E. Nigh for editing of the manuscript; U. Francke for karyotyping; A. Cherry and D. Bangs for help with fibroblast cultures; G. Panagiotakos and C. Young-Park for insightful discussions, and A. Krawisz, R. Schwemberger, D. Fu and R. Shu for help with data analysis. Antibodies to FORSE-1 were developed by P.H. Patterson and were obtained from the Developmental Studies Hybridoma Bank (University of Iowa). Financial support was provided by a US National Institutes of Health Director's Pioneer Award, and by grants to R.E.D. from the US National Institute of Mental Health, the California Institute for Regenerative Medicine and the Simons Foundation for Autism Research. S.P.P. was supported by awards from the International Brain Research Organization Outstanding Research Fellowship and the Tashia and John Morgridge Endowed Fellowship, M.Y. by a Japan Society of the Promotion for Science Postdoctoral Fellowship for Research Abroad and an American Heart Association Western States postdoctoral fellowship, T.P. by a Swiss National Science Foundation Postdoctoral Fellowship and A.S. by a California Institute for Regenerative Medicine Postdoctoral Fellowship. We are also grateful for funding from B. and F. Horowitz, M. McCafferey, B. and J. Packard, P. Kwan and K. Wang and the Flora foundation.

AUTHOR CONTRIBUTIONS

R.E.D. and S.P.P. designed the experiments and wrote the manuscript. S.P.P. generated iPSC lines, differentiated the iPSC lines into neurons, performed the calcium imaging and immunocytochemistry studies and contributed to the mutant mouse characterization. T.P. designed and analyzed the Fluidigm microarray studies. M.Y. generated and characterized the iPSC lines, and generated and characterized the mutant mice. I.V. and D.H.G. performed and analyzed the microarray gene expression experiments. A.S. derived neurons and designed and performed the electrophysiological experiments. A.M.P. performed the karyotyping and immunocytochemistry. S.C. and N.S. performed and analyzed catecholamine concentrations by HPLC. B.C. and T.D.P. contributed to the Fluidigm studies. J.A.B. and J.H. recruited and characterized the subjects.

COMPETING FINANCIAL INTERESTS

The authors declare no competing financial interests.

Published online at http://www.nature.com/naturemedicine/.
Reprints and permissions information is available online at http://www.nature.com/reprints/index.html.

1. Splawski, I. *et al.* Ca(V)1.2 calcium channel dysfunction causes a multisystem disorder including arrhythmia and autism. *Cell* **119**, 19–31 (2004).
2. Yarotskyy, V. *et al.* Roscovitine binds to novel L-channel (CaV1.2) sites that separately affect activation and inactivation. *J. Biol. Chem.* **285**, 43–53 (2010).
3. Yarotskyy, V. & Elmslie, K.S. Roscovitine, a cyclin-dependent kinase inhibitor, affects several gating mechanisms to inhibit cardiac L-type (Ca(V)1.2) calcium channels. *Br. J. Pharmacol.* **152**, 386–395 (2007).
4. Yarotskyy, V., Gao, G., Peterson, B.Z. & Elmslie, K.S. The Timothy syndrome mutation of cardiac CaV1.2 (L-type) channels: multiple altered gating mechanisms and pharmacological restoration of inactivation. *J. Physiol. (Lond.)* **587**, 551–565 (2009).
5. Wang, K. *et al.* Common genetic variants on 5p14.1 associate with autism spectrum disorders. *Nature* **459**, 528–533 (2009).
6. Moskvina, V. *et al.* Gene-wide analyses of genome-wide association data sets: evidence for multiple common risk alleles for schizophrenia and bipolar disorder and for overlap in genetic risk. *Mol. Psychiatry* **14**, 252–260 (2009).
7. Nyegaard, M. *et al.* CACNA1C (rs1006737) is associated with schizophrenia. *Mol. Psychiatry* **15**, 119–121 (2010).
8. Dolmetsch, R.E., Pajvani, U., Fife, K., Spotts, J.M. & Greenberg, M.E. Signaling to the nucleus by an L-type calcium channel-calmodulin complex through the MAP kinase pathway. *Science* **294**, 333–339 (2001).
9. Barrett, C.F. & Tsien, R.W. The Timothy syndrome mutation differentially affects voltage- and calcium-dependent inactivation of CaV1.2 L-type calcium channels. *Proc. Natl. Acad. Sci. USA* **105**, 2157–2162 (2008).
10. Takahashi, K. & Yamanaka, S. Induction of pluripotent stem cells from mouse embryonic and adult fibroblast cultures by defined factors. *Cell* **126**, 663–676 (2006).
11. Yu, J. *et al.* Induced pluripotent stem cell lines derived from human somatic cells. *Science* **318**, 1917–1920 (2007).
12. Yazawa, M. *et al.* Using induced pluripotent stem cells to investigate cardiac phenotypes in Timothy syndrome. *Nature* **471**, 230–234 (2011).
13. Zhang, S.C., Wernig, M., Duncan, I.D., Brustle, O. & Thomson, J.A. *In vitro* differentiation of transplantable neural precursors from human embryonic stem cells. *Nat. Biotechnol.* **19**, 1129–1133 (2001).
14. Pankratz, M.T. *et al.* Directed neural differentiation of human embryonic stem cells via an obligated primitive anterior stage. *Stem Cells* **25**, 1511–1520 (2007).
15. Li, X.J. *et al.* Coordination of sonic hedgehog and Wnt signaling determines ventral and dorsal telencephalic neuron types from human embryonic stem cells. *Development* **136**, 4055–4063 (2009).
16. Warren, L., Bryder, D., Weissman, I.L. & Quake, S.R. Transcription factor profiling in individual hematopoietic progenitors by digital RT-PCR. *Proc. Natl. Acad. Sci. USA* **103**, 17807–17812 (2006).
17. Flatz, L. *et al.* Single-cell gene-expression profiling reveals qualitatively distinct CD8 T cells elicited by different gene-based vaccines. *Proc. Natl. Acad. Sci. USA* **108**, 5724–5729 (2011).
18. Garbelli, R. *et al.* Layer-specific genes reveal a rudimentary laminar pattern in human nodular heterotopia. *Neurology* **73**, 746–753 (2009).
19. Saito, T. *et al.* Neocortical layer formation of human developing brains and lissencephalies: consideration of layer-specific marker expression. *Cereb. Cortex* **21**, 588–596 (2010).
20. Alcamo, E.A. *et al.* Satb2 regulates callosal projection neuron identity in the developing cerebral cortex. *Neuron* **57**, 364–377 (2008).
21. Britanova, O. *et al.* Satb2 is a postmitotic determinant for upper-layer neuron specification in the neocortex. *Neuron* **57**, 378–392 (2008).
22. Leone, D.P., Srinivasan, K., Chen, B., Alcamo, E. & McConnell, S.K. The determination of projection neuron identity in the developing cerebral cortex. *Curr. Opin. Neurobiol.* **18**, 28–35 (2008).
23. Pinto, D. *et al.* Functional impact of global rare copy number variation in autism spectrum disorders. *Nature* **466**, 368–372 (2010).
24. Garbett, K. *et al.* Immune transcriptome alterations in the temporal cortex of subjects with autism. *Neurobiol. Dis.* **30**, 303–311 (2008).
25. Ip, B.K., Bayatti, N., Howard, N.J., Lindsay, S. & Clowry, G.J. The corticofugal neuron-associated genes *ROBO1, SRGAP1* and *CTIP2* exhibit an anterior to posterior gradient of expression in early fetal human neocortex development. *Cereb. Cortex* **21**, 1395–1407 (2011).
26. Romano, G., Suon, S., Jin, H., Donaldson, A.E. & Iacovitti, L. Characterization of five evolutionary conserved regions of the human tyrosine hydroxylase (TH) promoter: implications for the engineering of a human TH minimal promoter assembled in a self-inactivating lentiviral vector system. *J. Cell. Physiol.* **204**, 666–677 (2005).
27. Raghanti, M.A. *et al.* Species-specific distributions of tyrosine hydroxylase–immunoreactive neurons in the prefrontal cortex of anthropoid primates. *Neuroscience* **158**, 1551–1559 (2009).
28. Dulcis, D. & Spitzer, N.C. Illumination controls differentiation of dopamine neurons regulating behaviour. *Nature* **456**, 195–201 (2008).
29. Barttfeld, P. *et al.* A big-world network in ASD: dynamical connectivity analysis reflects a deficit in long-range connections and an excess of short-range connections. *Neuropsychologia* **49**, 254–263 (2011).
30. Geschwind, D.H. & Levitt, P. Autism spectrum disorders: developmental disconnection syndromes. *Curr. Opin. Neurobiol.* **17**, 103–111 (2007).
31. Casanova, M.F. *et al.* Reduced gyral window and corpus callosum size in autism: possible macroscopic correlates of a minicolumnopathy. *J. Autism Dev. Disord.* **39**, 751–764 (2009).
32. D'Souza, A., Onem, E., Patel, P., La Gamma, E.F. & Nankova, B.B. Valproic acid regulates catecholaminergic pathways by concentration-dependent threshold effects on TH mRNA synthesis and degradation. *Brain Res.* **1247**, 1–10 (2009).
33. Toru, M., Nishikawa, T., Mataga, N. & Takashima, M. Dopamine metabolism increases in post-mortem schizophrenic basal ganglia. *J. Neural Transm.* **54**, 181–191 (1982).

ONLINE METHODS

iPSC maintenance. We cultured human iPSCs and the embryonic H9 line on irradiated four-drug-resistant (DR4) mouse embryonic fibroblast feeders.

Neural differentiation protocol. We carried out neural differentiation using a modified version of a previously described protocol[13]. Briefly, iPSCs were suspended to generate embryoid bodies and plated to produce neural rosettes (**Fig. 1a**, top). The rosettes were mechanically isolated and expanded as neurospheres and then either purified by FACS using the forebrain progenitor marker FORSE-1 (refs. 34,35) or plated for differentiation into neurons. Seven days after plating of the neurospheres, we observed cells expressing the mature form of MAP2 migrating away from the radial clusters of undifferentiated precursors expressing the dorsal forebrain marker PAX6 (**Fig. 1a**, middle). After 43 d of differentiation *in vitro*, we observed significant numbers of cells expressing the cortical marker DCX (**Supplementary Fig. 3**) and the mature form of MAP2 in the cultures (**Fig. 1a**, bottom). We performed five independent differentiations with four control lines, four Timothy syndrome lines, one 22q11 deletion syndrome line and one human embryonic stem cell line (H9). Each line was differentiated at least twice. In addition, we used two more control lines and one Timothy syndrome line for the rescue experiment (**Supplementary Table 1**). We dissolved R-Roscovitine (Sigma-Aldrich, R7772) in DMSO. We treated neuronal cultures with R-Roscovitine or with the same volume of DMSO at days 39 and 41. We analyzed the neuronal cultures at day 43 of differentiation.

Calcium imaging. We loaded NPCs (at passage two after plating of the neurospheres) or neuronal cultures at day 43 of differentiation with 1 μM Fura-2 acetoxymethyl ester (Invitrogen) for 30 min at 37 °C in Neurobasal/B27 medium, washed with Tyrode's solution and placed them in a perfusion chamber on the stage of an inverted fluorescence microscope (TE2000U; Nikon). We stimulated cells with high-KCl Tyrode's solution (67 mM KCl for neurons or 100 mM KCl for NPCs, 67 mM NaCl, 2 mM $CaCl_2$, 1 mM $MgCl_2$, 30 mM glucose and 25 mM HEPES, pH 7.4) without or with nimodipine (at a final concentration of 5 μM). We performed imaging at room temperature (23–25 °C) on an epifluorescence microscope equipped with an excitation filter wheel and an automated stage. We used Openlab software (PerkinElmer) to collect and quantify time-lapse excitation ratio images. We analyzed fluorescence images using IGOR Pro software (WaveMetrics).

Single-cell quantitative RT-PCR (qRT-PCR). We rinsed neuronal cultures at day 45 of differentiation with HBSS and incubated them with Accutase (Stemcell Technologies). After one wash with fresh Neurobasal medium (Invitrogen), we resuspended cells in Neurobasal/B27 medium containing 1 μg ml^{-1} propidium-iodide (Molecular Probes) and filtered them through a 40-μm nylon cell strainer (BD Biosciences). We performed clone sorting in 96-well qRT-PCR plates (Eppendorf) at the Stanford Shared FACS Facility on a BD Influx cell sorter. We sorted cells into 10 μl of pre-amplification mix containing 40 nM of all primers for the 96 genes of interest and the following components of the CellsDirect One-Step qRT-PCR Kit (Invitrogen): 2× Reaction Mix and SuperScript III RT/Platinum Taq Mix. After sorting, samples were reverse transcribed and pre-amplified for 18 cycles. We diluted (1:2) the pre-amplified samples with Tris EDTA buffer and stored them at −20 °C. Sample and assay (primer pair) preparation for the 96.96 Fluidigm Dynamic Arrays was done according to the manufacturer's recommendations. Briefly, we mixed the sample with 20× DNA Binding Dye Sample Loading Reagent (Fluidigm Corp.), 20× EvaGreen (Biotium) and TaqMan Gene Expression Master Mix (Applied Biosystems). Assays were mixed with 2× Assay loading reagent (Fluidigm Corp.) and Tris EDTA to a final concentration of 5 μM. We primed the 96.96 Fluidigm Dynamic Arrays (Fluidigm Corp.) and loaded on an IFC Controller HX (Fluidigm Corp.), and ran qRT-PCR experiments on a Biomark System for Genetic Anaylsis (Fluidigm Corp.). See the **Supplementary Methods** for details about the analysis.

Microarrays. We isolated RNA from fibroblasts, iPSCs, NPCs and neurons at rest or neurons stimulated with KCl (at day 43 of differentiation) using the RNeasy Mini kit and the RNase-Free DNase set (QIAGEN). Total RNA (200 ng) was amplified, labeled and hybridized on Illumina HumanRef-8 v3 Expression BeadChips (Illumina) according to the manufacturer's protocol. We analyzed data using the Lumi R[36] and Bioconductor (http://www.bioconductor.org/) packages, as previously described[37]. Briefly, absolute expression values were log2 transformed and normalized using quantile normalization. Data quality control measures included inter-array Pearson correlation, clustering based on the most variable genes (coefficient of variance >0.05) and detection of outlier arrays, as well as probe detection ($P < 0.05$). We performed differential expression analysis using a significance analysis of microarrays (http://www-stat.stanford.edu/~tibs/SAM/). The statistical criteria for differential expression were false discovery rate <0.05 and fold change >1.3.

Additional methods. Detailed methodology is described in the **Supplementary Methods**.

34. Elkabetz, Y. *et al.* Human ES cell-derived neural rosettes reveal a functionally distinct early neural stem cell stage. *Genes Dev.* **22**, 152–165 (2008).
35. Tole, S. & Patterson, P.H. Regionalization of the developing forebrain: a comparison of FORSE-1, Dlx-2, and BF-1. *J. Neurosci.* **15**, 970–980 (1995).
36. Du, P., Kibbe, W.A. & Lin, S.M. lumi: a pipeline for processing Illumina microarray. *Bioinformatics* **24**, 1547–1548 (2008).
37. Coppola, G. *et al.* Gene expression study on peripheral blood identifies progranulin mutations. *Ann. Neurol.* **64**, 92–96 (2008).